

# Two-Mode Stochastic Magnetic Structure in Nanocrystalline Soft Magnetic Fe–Zr Films

Eugene V. Harin,\* Elena N. Sheftel, Valentin A. Tedzhetov,  
and Galina S. Usmanova

The magnetic structure of Fe<sub>100-x</sub>Zr<sub>x</sub> films ( $x = 0, 0.6, 1.8, 2.9$ , and  $4.1 \pm 0.1$  at%), which is characterized by the existence of stochastic domains determined by correlation magnetometry method, is discussed in terms of the random anisotropy model. It is found that two modes of the magnetic anisotropy field of stochastic domains are formed, which differ in the exchange stiffness magnitude and determine the existence of two modes of the coercive field found in the magnetic hysteresis loops.

## 1. Introduction

Nanocrystalline and amorphous ferromagnetic alloys are able to combine outstanding soft magnetic properties.<sup>[1]</sup> The hysteresis properties of such alloys can be most fully explained using random anisotropy model (RAM).<sup>[2]</sup> This model assumes that axes of easy magnetization of individual grains of radius  $R_c$  (or local ferromagnetically homogeneous regions of radius  $R_c$  in an amorphous phase) are randomly oriented and exchange interaction is possible between grains. Therefore, the distribution of local magnetic moments of  $2R_c$  can be described by some autocorrelation function.<sup>[3]</sup> An important parameter of this function is the magnetic autocorrelation radius  $R_L$ , it is the size of region in which the magnetization is relatively homogeneous as the result of competition between exchange interaction and magnetic anisotropy.

In nano- and amorphous alloys, an extreme decrease in the coercive field regarding the local magnetic anisotropy field ( $H_c \ll H_a$ ) is realized under the condition  $R_L \gg R_c$ . This condition exists in RAM in the case when the length of the exchange interaction exceeds the size of  $R_c$ , which causes averaging of the local magnetic anisotropy in the volume of radius  $R_{L1}$  (stochastic magnetic domain).<sup>[2,3]</sup>

The above case assumes the size of the magnetic anisotropy inhomogeneities of the grain size order and the uniform exchange energy; however, both can have the size of inhomogeneity greater than the grain size. Such inhomogeneities of exchange energy were detected by spin-wave spectroscopy.<sup>[4]</sup> The

effect of such inhomogeneities on the magnetization curve for the case of one-dimensional chain of grains was theoretically considered in ref. [5]. It can be assumed, under certain conditions, that there may be some other reasons for the existence of a second magnetic autocorrelation radius  $R_{L2}$  (a second stochastic magnetic domain) in the material. Note that the simultaneous existence of two modes of stochastic domains has not yet been observed experimentally.

Fe<sub>100-x</sub>Zr<sub>x</sub> alloys are known for the diversity of their magnetic properties<sup>[6]</sup> and are a convenient material for studying the effect of phase composition and crystal structure<sup>[7]</sup> on the magnetic structure and magnetic properties.<sup>[8]</sup>

This paper presents the results pointing out the correlation of two coercive fields with two magnetic autocorrelation radii in the nanocrystalline Fe–Zr films.

## 2. Experimental Section

The Fe<sub>100-x</sub>Zr<sub>x</sub> films were obtained by dc magnetron sputtering of targets consisting of a Fe disk with a diameter of 100 mm and Zr chips  $3 \times 3 \times 1$  mm in size evenly distributed over the erosion zone (5 compositions: from 0 to 12 Zr chips with an increment of 3 chips). Deposition parameters: residual vacuum  $6.27 \times 10^{-3}$  Pa, Ar pressure 0.68 Pa, current 1 A, voltage 300 V, deposition time 40 min. The thickness of the films, measured on a Fischerscope X-ray fluorescence spectrometer, is  $1.5 \pm 0.1$   $\mu$ m. Here and further, confidence interval is determined by  $\pm \Delta = 1.96[\sum(a_i - a_{\text{mean}})^2]^{1/2}/n$ , where  $n$  is amount of value  $a_i$  measurements,  $a_{\text{mean}}$  is arithmetic mean value of  $a_i$ . Glass plates 1.5 mm thick were used as substrates.

The chemical composition of the films was determined by energy dispersive X-ray spectroscopy using a Hitachi TM3000 scanning electron microscope with a Bruker Quantax 70 EDS attachment. The Zr content was 0, 0.6, 1.8, 2.9, and  $4.1 \pm 0.1$  at%.

Studies of the phase-structural state were performed by X-ray diffractometry (XRD) using a Rigaku Ultima IV diffractometer equipped with a graphite monochromator in Bragg-Bretano geometry using CuK $\alpha$  radiation. Scintillation and semiconductor detectors were used to record the radiation. For the initial processing of experimental data, qualitative and quantitative phase analysis, a package of original programs was used,<sup>[9]</sup> using full-profile analysis by the Rietveld method. XRD patterns were used to determine the phase composition (the volume fractions

Dr. E. V. Harin, Prof. E. N. Sheftel, V. A. Tedzhetov,  
Dr. G. S. Usmanova  
Baikov Institute of Metallurgy and Materials Science RAS  
Leninsky pr. 49, Moscow 119334, Russia  
E-mail: ekharin@imet.ac.ru

of crystalline phases), the lattice parameters of the phases, and the fine structure of the films (the size of the coherent scattering region corresponding to a grain diameter of  $2R_c$ ).

Magnetization curves and hysteresis loops were measured on a LakeShore 7407 vibration magnetometer in fields up to 16 kOe. The parameters of the magnetic structure are determined by the method of correlation magnetometry.<sup>[3,10–12]</sup> All measurements were performed at room temperature.

### 3. Results and Discussion

According to XRD (Figure 1a), all films contain only the  $\alpha$ -Fe phase, the lattice parameter of this phase monotonously increases from 2.87 to  $2.924 \pm 0.003$  Å with Zr content increasing (Figure 1b), which indicates the formation of a solid solution of Zr in  $\alpha$ -Fe. The seeming decrease of the lattice parameter from  $2.928 \pm 0.003$  Å at 2.9 at% Zr to  $2.924 \pm 0.003$  Å at 4.1 at% Zr lies in the confidence interval  $\pm 0.003$  Å and may indicate the saturation of a solid solution of Zr in  $\alpha$ -Fe. The grain size simultaneously decreases from 10 to  $4 \pm 2$  nm (Figure 1c), which is also a consequence of solid solution formation. The absence of Zr-containing phases in the films, despite the content of Zr up to 4 at%, is, on the one hand, due to the dissolution of Zr in  $\alpha$ -Fe, and on the other hand, can be explained by the insufficient sensitivity of the XRD method for the identification of phases with a volume fraction less than 10 vol%.

The saturation magnetization  $M_s$  and the coercive field  $H_c$  (Figure 2) decrease monotonically with increasing

Zr content (from  $1620 \pm 110$  to  $1290 \pm 60$  G and from  $200 \pm 10$  to  $9 \pm 1$  Oe, respectively). In accordance with RAM,<sup>[2]</sup> the coercive field of the studied films follows the relation for the grain size  $H_c \approx (2R_c)^6$ , which is shown in Figure 2b by solid line.

The shapes of hysteresis loops of the studied films indicate the presence of two modes of magnetic anisotropy in them. This fact is indicated by a “step” in a field about  $H_c$  (Figure 3a). To determine the coercive field of each of the magnetic anisotropies ( $H_{c1}$  and  $H_{c2}$ ), the loops were described by the empirical function (1) which can be considered as the modification of classical Langevin formula for magnetization process.<sup>[11]</sup> The experimentally determined magnetization (open symbols in Figure 3a) is the algebraic sum of magnetization values corresponding to two hysteresis loops:

$$M(H) = M_{s1} V_1 (\text{cth}(P_1(H \pm H_{c1})) - (P_1(H \pm H_{c1}))^{-1}) + M_{s2} V_2 (\text{cth}(P_2(H \pm H_{c2})) - (P_2(H \pm H_{c2}))^{-1}) + \chi H \quad (1)$$

where  $P_1$ ,  $P_2$ ,  $M_{s1} V_1$ ,  $M_{s2} V_2$ , and  $\chi$  are the adjustable parameters. Note that the hysteresis loop is the magnetic moment of the sample divided by its volume. If there are two phases in a film with different saturation magnetizations, they are summed in proportion to their volume fractions  $V_1$  and  $V_2$ . Since XRD gave us information about only one ferromagnetic phase, it is impossible to distinguish saturation magnetizations, that is,  $M_{s1}$  and  $M_{s2}$  cannot be identified with specific quantities.

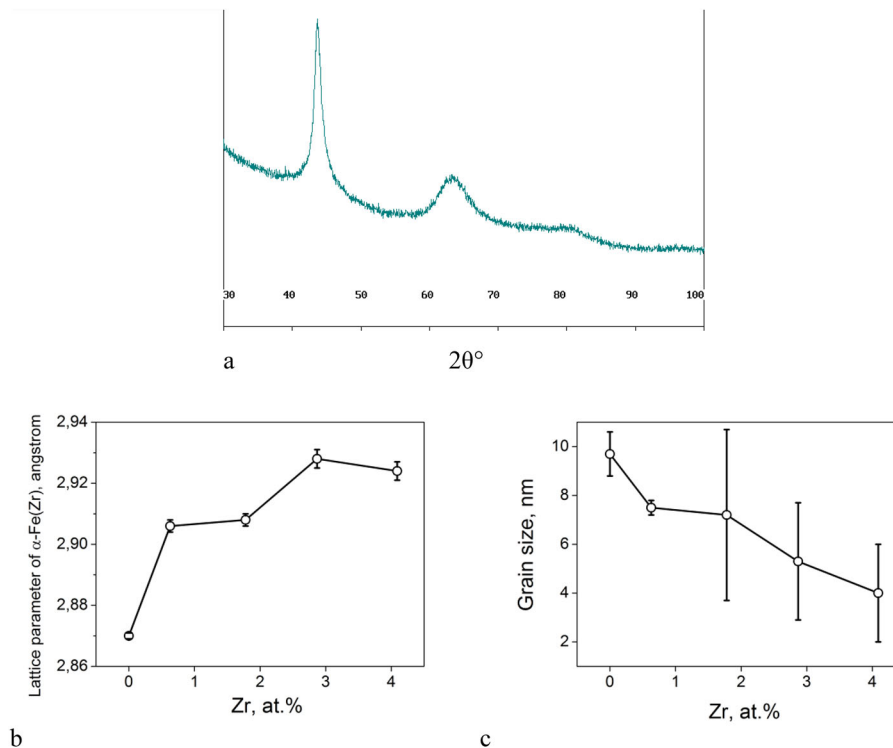


**Figure 1.** XRD pattern of the  $\text{Fe}_{95.9}\text{Zr}_{4.1}$  film (a); dependence of the lattice parameter (b) and the grain size (c) of  $\alpha$ -Fe on the Zr concentration in the  $\text{Fe}_{100-x}\text{Zr}_x$  films. The lines are guides for the eyes.

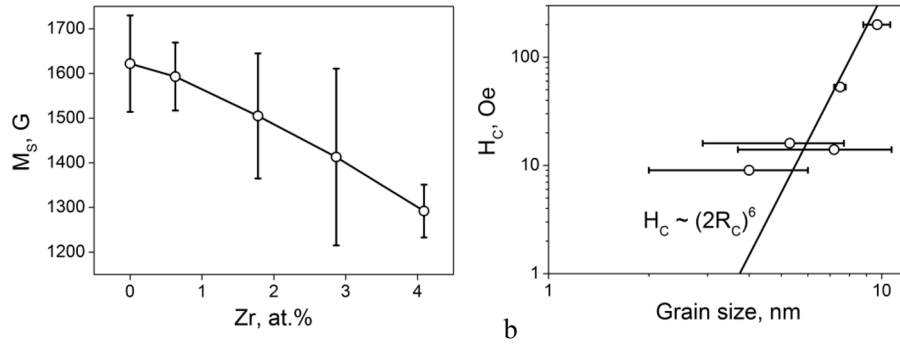


**Figure 2.** Dependences of saturation magnetization on Zr concentration (a) and coercive field on the grain size of  $\alpha$ -Fe phase (b) in the  $\text{Fe}_{100-x}\text{Zr}_x$  films. The line on (a) is guide for the eyes.

The magnetization curves of the studied films in the strong fields are fitted by the law of approaching to saturation magnetization<sup>[10,11]</sup>

$$M(H) = M_s [1 - (1/2)(D^{1/2}H_a)^2 / (H^2 + H^{1/2}H_R^{3/2})] \quad (2)$$

from which the saturation magnetization  $M_s$ , the rms fluctuation of the local (on the ferromagnetic grain scale) magnetic anisotropy field  $D^{1/2}H_a$  ( $D$  is dispersion of local anisotropy axes,<sup>[3]</sup> which is unknown in this study) and exchange field  $H_R$  ( $H_R = 2A/M_s R_c^2$ , where  $A$  is exchange stiffness and  $R_c$  is grain radius, Figure 1c) are determined.

$D^{1/2}H_a$  values for all studied films are lower than the exchange field  $H_R$ . According to ref. [3], the exchange field is a threshold value of  $D^{1/2}H_a$ , below which ( $D^{1/2}H_a < H_R$ ) the exchange interaction results in the formation of stochastic domains. Thus, the magnetic structure formed in the studied films consists of stochastic domains.

Using estimated  $D^{1/2}H_a$  and  $H_R$  values, the value of the 1st mode of anisotropy field of stochastic domains  $D^{1/2}\langle H_a \rangle_1$ <sup>[13,14]</sup> and their relative size  $R_{L1}/R_c$ <sup>[14]</sup> were determined by

$$D^{1/2}\langle H_a \rangle_1 = (D^{1/2}H_a)^4 / H_R^3 \quad (3)$$

$$R_{L1}/R_c = (H_R / D^{1/2}H_a)^2 \quad (4)$$

It should be noted that the obtained inequality  $R_{L1}/R_c > 1$  for the studied films indicates the correctness of the consideration of their magnetic structure in terms of RAM.<sup>[2,3]</sup>

Correlation magnetometry method<sup>[3,12]</sup> provides an opportunity to determine the  $D^{1/2}H_a$  and  $H_R$  parameters also by the graphical analysis of the magnetization dispersion  $d_m = 1 - M/M_s$  dependence on the external field  $H$ , which is plotted on log-log scale (Figure 3b). Here, line I, described by Equation (2), has two asymptotes: II is described by  $d_m = (1/2)(D^{1/2}H_a/H)^2$  (Akulov's law); III is described by  $d_m = (1/2)(D^{1/2}H_a)^2 / (H_R^{3/2}H^{1/2})$  (the decrease in the stochastic domain size with increasing field), from which the  $D^{1/2}H_a$  and  $H_R$  values can be determined.  $H_R$  is a field of intersection of the asymptotes II and III. Asymptote IV corresponding to a field range below about 100 of oersteds is described by<sup>[12]</sup>

$$d_m = (1/2)(D^{1/2}\langle H_a \rangle_2 / H)^2 \quad (5)$$

$H_L$  is a field of intersection of the asymptotes III and IV.

Using Equation (5), the 2nd mode of anisotropy field of stochastic domains  $D^{1/2}\langle H_a \rangle_2$  was determined. As it is seen from Figure 4, the  $D^{1/2}\langle H_a \rangle_1$  values exceed  $D^{1/2}\langle H_a \rangle_2$  by a few orders of magnitude. The fields  $D^{1/2}\langle H_a \rangle_1$  and  $D^{1/2}\langle H_a \rangle_2$  correlate well with coercive fields  $H_{c1}$  and  $H_{c2}$  (Figure 4).

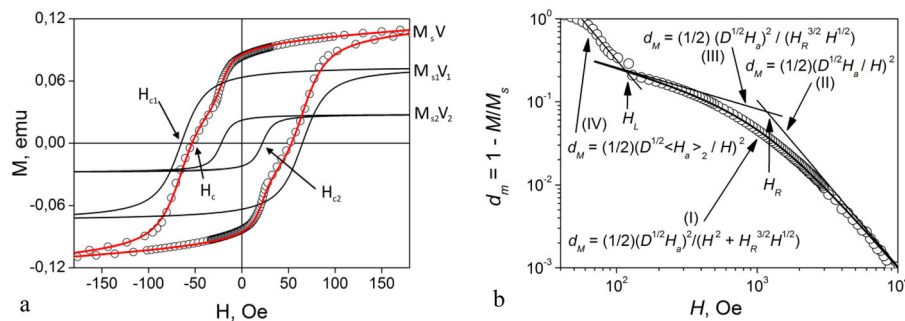


**Figure 3.** a) Hysteresis loop of the  $\text{Fe}_{99.4}\text{Zr}_{0.6}$  film and its fitting by Equation (1). b) Magnetization dispersion of the  $\text{Fe}_{99.4}\text{Zr}_{0.6}$  film and its description by the method of correlation magnetometry.

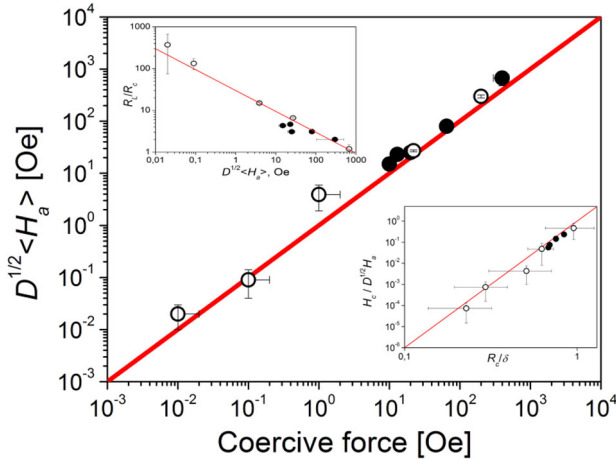


**Figure 4.** The parameters of the stochastic domains in the studied films:  
• –  $H_{c1} = D^{1/2} \langle H_a \rangle_1$ ,  $R_{L1}/R_c \approx (D^{1/2} \langle H_a \rangle_1)^{-1/2}$ ,  $H_{c1}/(D^{1/2} H_a) \approx R_c/\delta_1$ ;  
○ –  $H_{c2} = D^{1/2} \langle H_a \rangle_2$ ,  $R_{L2}/R_c \approx (D^{1/2} \langle H_a \rangle_2)^{-1/2}$ ,  $H_{c2}/(D^{1/2} H_a) \approx R_c/\delta_2$ .

When assuming that the field  $D^{1/2} \langle H_a \rangle_2$  is determined for an area with the relative size<sup>[15]</sup>

$$R_{L2}/R_c = \left( H_R / D^{1/2} \langle H_a \rangle_2 \right)^{1/2} \quad (6)$$

it follows that  $R_{L2}/R_c > R_{L1}/R_c > 1$  (the left inset on Figure 4; the solid line is  $R_L/R_c = (H_R / D^{1/2} \langle H_a \rangle)^{1/2}$  indicating that all stochastic domains have comparable  $H_R$  values). It is assumed that average effective parameters  $2R_c$ ,  $M_s$ , and  $D^{1/2} H_a$  remain unchanged over the entire film volume (i.e., two modes of stochastic domains have the same  $2R_c$ ,  $M_s$ , and  $D^{1/2} H_a$ , which follows from the XRD data and the fitting of magnetization curves by Equation (2)).

In terms of RAM when the coercive field is determined only by exchange interaction between grains (the magnetization process is realized via the stochastic domain magnetization rotation,  $H_c = D^{1/2} \langle H_a \rangle$ ), the value of coercive field is described by the expression<sup>[2]</sup>

$$H_c \approx K_{\text{eff}}^4 (2R_c)^6 / (M_s A^3) \quad (7)$$

For convenience, this relation can be transformed to the form<sup>[12]</sup>

$$H_c / D^{1/2} H_a = (R_c / \delta)^6 \quad (8)$$

where  $\delta = (A/K)^{1/2}$ ,  $K = H_a M_s / 2$ . The  $R_c/\delta$  ratio can be determined directly from the results obtained by Equation (2):  $R_c/\delta = (R_L/R_c)^{-1/4}$ . The dependence  $H_c / D^{1/2} H_a = (R_c/\delta)^6$  was successfully checked by an example of nine different alloys.<sup>[12]</sup>

For the studied  $\text{Fe}_{100-x}\text{Zr}_x$  films, the correlation between  $H_c / D^{1/2} H_a$  and  $R_c/\delta$  is shown in the right inset in Figure 4 (the solid line is  $H_c / D^{1/2} H_a = (R_c/\delta)^6$ , which is identical to  $H_c = D^{1/2} \langle H_a \rangle$ ). The found correlations  $H_{c1}/D^{1/2} H_a \approx R_c/\delta_1$  and  $H_{c2}/D^{1/2} H_a \approx R_c/\delta_2$  mean that both coercive fields ( $H_{c1}$  and  $H_{c2}$ ) satisfy RAM, i.e., both modes of the stochastic-domain anisotropy field result from the exchange interaction between grains.

Taking into account the fact that the  $M_s$ ,  $D^{1/2} H_a$ , and  $R_c$  magnitudes are identical for both stochastic-domain modes, the different magnitudes of exchange stiffness  $A$  (in  $\delta = (A/K)^{1/2}$ ) are the cause of the formation of both domain modes. The obtained results allow us to assume that a magnetic structure formed in the films is related to the presence of two ferromagnetic phases differing in the solid solution composition (and therefore in  $A$  values), which cannot be distinguished by XRD.

## 4. Summary

The dc magnetron sputtering was used to prepare nanocrystalline  $\text{Fe}_{100-x}\text{Zr}_x$  films ( $x = 0, 0.6, 1.8, 2.9$ , and  $4.1 \pm 0.1 \text{ at\%}$ ); the phase composition of the films is the  $\alpha$ -Fe-based solid solution supersaturated with zirconium, with grain size of 4–10 nm. The formation of a solid solution of Zr in the  $\alpha$ -Fe, confirmed by the concentration dependence of the lattice parameter of the  $\alpha$ -Fe phase, affects the inhibition of nanocrystalline grain growth (a solid solution strengthening), which is reflected in a decrease in grain size of the  $\alpha$ -Fe phase with increasing Zr content in the films. Zr-containing phases are not identified in the  $\text{Fe}_{100-x}\text{Zr}_x$  films due to the introduction of Zr into the  $\alpha$ -Fe solid solution and, possibly, due to the insufficient sensitivity of the XRD method. The saturation magnetization  $M_s$  and the coercive field  $H_c$  monotonously decrease with increasing Zr content (from 1600 to 1300 G and from 200 to 9 Oe, respectively), which for the latter is a consequence of RAM. The shapes of magnetic hysteresis loops indicate the presence of two main modes of coercive field in the studied  $\text{Fe}_{100-x}\text{Zr}_x$  films. The magnetic structure of the films, which is characterized by the existence of stochastic domains, is discussed in terms of RAM. The correlation magnetometry method was used to determine the parameters of the local (the magnetic anisotropy field within a grain  $D^{1/2} H_a$ ) and macroscopic magnetic structure (the magnetic anisotropy field within a stochastic domain  $D^{1/2} \langle H_a \rangle$  and the stochastic domain radius  $R_L$ ). It was found that two modes of the magnetic anisotropy field of stochastic domains  $D^{1/2} \langle H_a \rangle_1$  and  $D^{1/2} \langle H_a \rangle_2$  are formed, which differ in the exchange stiffness magnitude and determine the existence of two coercive fields.

## Acknowledgments

The reported magnetic measurements and analysis were funded by RFBR according to the research project no. 18-32-00485mol\_a ("Effective parameters of magnetic structure in nanocrystalline ferromagnetic bcc Fe-based films"). The reported XRD analysis was funded by the state order according to no. 075-00746-19-00.

## Conflict of Interest

The authors declare no conflict of interest.

## Keywords

correlation magnetometry, magnetic materials, nanocrystalline materials, random anisotropy model, thick films

Received: February 1, 2019

Revised: March 19, 2019

Published online:

- 
- [1] F. Fiorillo, G. Bertotti, C. Appino, M. Pasquale, in *Wiley Encyclopedia of Electrical and Electronics Engineering* (Ed. J. G. Webster), Vol. 19, John Wiley & Sons, Hoboken, NJ **2016**.
  - [2] G. Herzer, *Acta Mater.* **2013**, 61, 718.
  - [3] R. S. Iskhakov, S. V. Komogortsev, *Phys. Met. Metallogr.* **2011**, 112, 666.
  - [4] B. P. Khrustalev, A. D. Balaev, V. G. Pozdnyakov, L. I. Vershinina, *Solid State Commun.* **1985**, 55, 657.
  - [5] S. Komogortsev, S. Smirnov, R. Iskhakov, N. Momot, A. Balaev, L. Chekanova, E. Denisova, E. Eremin, *Solid State Phenomena* **2011**, 168–169, 369.
  - [6] D. Goll, R. Loeffler, U. Pflanz, T. Gross, G. Schneider, *Phys. Status Solidi RRL* **2018**, 12, 1700221.
  - [7] P. Gorria, J. S. Garitaonandia, M. J. Pérez, J. A. Blanco, J. Campo, *Phys. Status Solidi RRL* **2009**, 3, 28.
  - [8] R. S. Iskhakov, M. M. Brushtunov, A. G. Narmonev, I. A. Turpanov, L. A. Chekanova, *Fiz. Met. Metalloved.* **1995**, 79, 122.
  - [9] E. V. Shelekhov, T. A. Sviridova, *Met. Sci. Heat Treat.* **2000**, 42, 309.
  - [10] S. V. Komogortsev, R. S. Iskhakov, *J. Magn. Magn. Mater.* **2017**, 440, 213.
  - [11] S. V. Komogortsev, E. A. Denisova, R. S. Iskhakov, A. D. Balaev, L. A. Chekanova, Yu. E. Kalinin, A. V. Sitnikov, *J. Appl. Phys.* **2013**, 113, 17C105.
  - [12] R. S. Iskhakov, S. V. Komogortsev, *Bull. Russ. Acad. Sci. Phys.* **2007**, 71, 1620.
  - [13] E. M. Chudnovsky, *J. Appl. Phys.* **1988**, 64, 5770.
  - [14] R. S. Iskhakov, S. V. Komogortsev, Z. M. Moroz, E. E. Shalygina, *JETP Lett.* **2000**, 72, 603.
  - [15] R. S. Iskhakov, V. A. Ignatchenko, S. V. Komogortsev, A. D. Balaev, *JETP Lett.* **2003**, 78, 646.